Optica Applicata, Vol. XXXVIII, No. 4, 2008

Skew ray tracing and error analysis of optical elements with ellipsoid boundary surfaces

TE-TAN LIAO

Department of Mechanical Engineering, Far East University,
No. 49, Chung Hua Road, Hsin-Shih. Tainan 744, Taiwan; e-mail: ttliao@cc.feu.edu.tw

Utilizing a ray tracing approach based upon Snell's optical laws and a 4×4 homogeneous coordinate transformation matrix, this study conducts a systematic analysis of the errors induced in the paths of skew rays as they pass through an optical element with an ellipsoid boundary surface. The error analysis performed in this study considers two principal sources of light path error, namely (1) translational and rotational errors of the boundary surfaces, and (2) differential changes induced in the position of the incident ray on the boundary surface and the unit directional vector of the refracted/reflected ray as a result of changes in the position and unit directional vector of the light source. The validity of the proposed methodology is demonstrated by analyzing an optical element with an arbitrary ellipsoid boundary surface.

Keywords: skew ray tracing, error analysis, ellipsoid boundary surface.

1. Introduction

In general, the light rays within an optical system can be classified as either axial, meridional or skew [1]. Evaluating the performance of optical systems during their theoretical design stage requires the ability to determine the paths of these light rays as they undergo successive reflection and refraction events at the boundaries of the various optical elements within the system. This is generally achieved using a ray tracing procedure in which Snell's laws of reflection and refraction are applied at each boundary surface encountered by the rays. Whilst this process is relatively straightforward for the axial or meridional rays within the system, tracing the paths of skew rays is more problematic since such rays propagate in an arbitrary plane and their precise point of incidence upon the boundary surface is unknown. Nonetheless, their paths must be traced if the performance of the optical system is to be reliably evaluated.

Due to the limitations of traditional manufacturing techniques, the lenses and mirrors used in many optical systems have a simple planar or spherical form. However, this limits the performance of the optical system and thus considerable effort has been expended in developing aspherical lenses in recent decades. Compared to their planar or spherical counterparts, aspherical lenses are both smaller and lighter and tend to provide an im-

proved optical performance. Furthermore, in some instances, the use of aspherical elements facilitates the construction of optical systems with fewer lens components, thereby achieving significant size and weight savings [2]. For example, the Gregorian two-mirror system formed with a concave parabolic primary mirror and a concave elliptical secondary mirror has been popular as a small erecting telescope for terrestrial observation [3].

Ray tracing provides a powerful technique for analyzing the performance of optical lenses, and is an essential task when designing and analyzing optical systems. The traced ray set generally includes the rays which start at a given set of object points and pass through a given set of points on the aperture stop [4]. In the differential ray tracing process, the effects of each optical component are evaluated by differentiating the equations relating the configuration of the rays before and after their transformation at the component surface [5, 6]. However, tracing the paths of skew rays as they pass through an aspherical surface is difficult since the precise point of intersection with the aspherical surface cannot be determined directly. Nonetheless, SMITH [1] successfully developed an iterative technique for performing aspherical-boundary skew ray tracing based upon a series of approximations which continued until the approximation error converged to a negligible value. Ray tracing approaches enable the sensitivity of an optical system to design or manufacturing flaws to be assessed by relating the differential changes of the reflected or refracted rays at a boundary surface to differential changes of the incident ray. Such a technique allows the contribution of each boundary surface within the optical system to be systematically examined. A sensitivity analysis also enables the establishment of fundamental aberration functions, which simplify the task of determining the effects of optical aberrations on the overall performance of an optical system [7, 8]. Furthermore, sensitivity analysis allows the orientation of an image to be accurately determined. For example, TSAI and LIN [9] applied the results of a sensitivity analysis to construct a merit function describing the change in orientation of an image as it was successively reflected/refracted at a series of flat boundary surfaces within a prism.

The image quality of an optical system is governed primarily by the flaws and assembly errors of its individual elements [10]. In designing and evaluating the image quality of an optical system, an analogy can be drawn with the design of a NC (numerical control) machine tool since in the same way that optical systems are composed of a series of individual optical elements, machine tools comprise a structured arrangement of interconnected links and joints, each having a unique set of resolution characteristics. When designing a machine tool, it is necessary to identify the potential sources of error within the system and to clarify their individual and collective effects on the overall quality of the machined products. In an early study TLUSTY [11] showed that the machining error of a NC machine tool varies as a function of the combined effects of the individual errors in each of its six degrees of freedom. Accordingly, FERREIRA and LIU [12] developed a model based upon three rotational errors, *i.e.*, $\Delta\Gamma_i$, $\Delta\Psi_i$ and $\Delta\Phi_i$, and three translational errors, *i.e.*, Δx_i, Δy_i and Δz_i, to enable the performance of a machine tool to be systematically examined.

In a previous study [13], the current author drew an analogy with the error model presented in [12] to develop a skew ray sensitivity analysis model with which it is pos-

sible to analyze the errors induced in a ray's light path as it was reflected and/or refracted at a flat optical boundary surface. The proposed model considered the effects of six sources of light path error (*i.e.*, three translational errors and three rotational errors) on the deviation of the light path at the boundary surface. Furthermore, the effects of changes in the incident position and unit directional vector of the refracted/reflected ray caused by changes in the position and unit directional vector of the light source were also examined. In the current study, this model is extended to analyze the errors induced in the paths of skew rays incident upon an ellipsoid boundary surface.

In performing the ray tracing analysis, a 4×4 homogeneous transformation matrix is used to define the position and orientation of the local coordinate frame of each boundary surface. The reflection/refraction paths of the incident rays are then determined using Snell's conventional optical laws. In the analysis, a position vector $P_{ix}\mathbf{i} + P_{iy}\mathbf{j} + P_{iz}\mathbf{k}$ is written as a column matrix ${}^{j}P_i = [P_{ix} \quad P_{iy} \quad P_{iz} \quad 1]^T$, where the pre-superscript j of the leading symbol ${}^{j}P_i$ indicates that this vector is referred with respect to coordinate frame $(xyz)_j$. Given a point ${}^{j}P_i$, its transformation ${}^{k}P_i$ is represented by the matrix product ${}^{k}P_i = {}^{k}A_i {}^{j}P_i$, where ${}^{k}A_j$ is a 4×4 matrix defining the position and orientation (referred to hereafter as the configuration) of a frame $(xyz)_j$ with respect to another frame $(xyz)_k$ [14]. The same notation rules are also applicable to the unit directional vector ${}^{j}\ell_i = [\ell_{ix} \quad \ell_{iy} \quad \ell_{iz} \quad 0]^T$. Note that if a vector is referred to the world coordinate frame $(xyz)_j$, its pre-superscript 0 is omitted for reasons of simplicity.

The remainder of this paper is organized as follows. Section 2 describes the use of the 4×4 homogeneous transformation matrix and Snell's optical laws to perform skew ray tracing at an ellipsoid boundary surface, while Section 3 develops the corresponding error analysis methodology. Section 4 demonstrates the application of the proposed approach to the error analysis of an arbitrary optical element with a refractive ellipsoid boundary surface. Finally, Section 5 presents some brief concluding remarks and indicates the intended direction of future research.

2. Skew ray tracing at ellipsoid boundary surface

A fundamental feature of optical elements with planar, spherical or aspherical boundary surfaces is that these surfaces are all surfaces of revolution. Consequently, the error analysis methodology proposed in this study commences by defining the boundary surface in terms of revolution geometry and then applies a ray tracing technique to establish the paths followed by skew rays as they undergo reflection and refraction at this surface. The error analysis methodology developed in this study is applicable to all rotationally-symmetric optical elements, including both spherical and aspherical (*e.g.*, paraboloidal, ellipsoid and hyperboloid). However, in defining these surfaces in terms of revolution geometry, the parameterized form of the generating curve is different in every case. The current study therefore considers the specific case of an ellipsoid boundary surface for illustration purposes.

As shown in Fig. 1, the boundary surface ${}^{i}r_i$ of an ellipsoid optical element can be obtained by rotating the generating line ${}^{i}q_i = [a_iC\beta_i \;\; 0 \;\; b_iS\beta_i \;\; 1]^T$, where $a_i, b_i \geq 0$, $a_i \neq b_i$ and $-\frac{\pi}{2} \leq \beta_i \leq \frac{\pi}{2}$, in the x_iz_i plane about the z_i axis, i.e.

$$ {}^{i}r_i = \mathrm{Rot}(z_i, \alpha_i)\,{}^{i}q_i = \begin{bmatrix} C\alpha_i & -S\alpha_i & 0 & 0 \\ S\alpha_i & C\alpha_i & 0 & 0 \\ 0 & 0 & 1 & 0 \\ 0 & 0 & 0 & 1 \end{bmatrix} \begin{bmatrix} a_iC\beta_i \\ 0 \\ b_iS\beta_i \\ 1 \end{bmatrix} = [a_iC\beta_iC\alpha_i \quad a_iC\beta_iS\alpha_i \quad b_iS\beta_i \quad 1]^T \tag{1} $$

where $\mathrm{Rot}(z_i, \alpha_i)$ is the rotation transformation matrix about the z_i axis and C and S denote cosine and sine functions, respectively. Equation (1) provides a generic expression for parametrizing the boundaries of optical elements with ellipsoid surfaces in terms of a_i, b_i and the polar angular position α_i, β_i. The unit normal vector ${}^{i}n_i$ $\left({}^{i}n_i = s_i \left(\frac{\partial {}^{i}r_i}{\partial \beta_i} \times \frac{\partial {}^{i}r_i}{\partial \alpha_i} \right) \Big/ \left| \frac{\partial {}^{i}r_i}{\partial \beta_i} \times \frac{\partial {}^{i}r_i}{\partial \alpha_i} \right| \right)$ along the boundary surface ${}^{i}r_i$ is given as

$$ {}^{i}n_i = s_i \left[\frac{b_iC\beta_iC\alpha_i}{\sqrt{a_i^2(S\beta_i)^2 + b_i^2(C\beta_i)^2}} \quad \frac{b_iC\beta_iS\alpha_i}{\sqrt{a_i^2(S\beta_i)^2 + b_i^2(C\beta_i)^2}} \quad \frac{a_iS\beta_i}{\sqrt{a_i^2(S\beta_i)^2 + b_i^2(C\beta_i)^2}} \quad 0 \right]^T \tag{2} $$

where s_i is specified as either +1 or –1 such that the cosine of the incident angle has a positive value, *i.e.*, $C\theta_i > 0$. Having obtained general expressions for ${}^{i}n_i$ and ${}^{i}r_i$, any skew ray can be traced simply by applying Snell's optical laws of reflection and refraction.

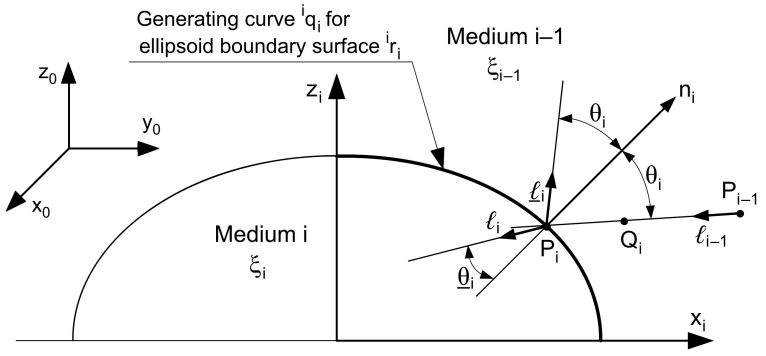

Fig. 1. Boundary formed by rotating surface geometry and skew ray tracing at ellipsoid boundary surface.

In the derivations above, ${}^{i}r_i$ and ${}^{i}n_i$ are both expressed with respect to the ellipsoid boundary surface coordinate frame $(xyz)_i$. The relative configuration of the world frame $(xyz)_0$ with respect to frame $(xyz)_i$ is given by

$$ {}^{i}A_0 = A_{i0} = \begin{bmatrix} I_{ix} & J_{ix} & K_{ix} & t_{ix} \\ I_{iy} & J_{iy} & K_{iy} & t_{iy} \\ I_{iz} & J_{iz} & K_{iz} & t_{iz} \\ 0 & 0 & 0 & 1 \end{bmatrix} \tag{3} $$

where vectors $[I_{ix} \quad I_{iy} \quad I_{iz} \quad 0]^T$, $[J_{ix} \quad J_{iy} \quad J_{iz} \quad 0]^T$ and $[K_{ix} \quad K_{iy} \quad K_{iz} \quad 0]^T$ describe the orientations of the three unit vectors of frame $(xyz)_0$ with respect to frame $(xyz)_i$, and vector and $[t_{ix} \quad t_{iy} \quad t_{iz} \quad 1]^T$ is the position vector of the origin of frame $(xyz)_0$ with respect to frame $(xyz)_i$. The unit normal vector of the ellipsoid boundary surface referred to frame $(xyz)_0$ can be obtained by transforming ${}^{i}n_i$ to frame $(xyz)_0$, *i.e.*

$$ n_i = \begin{bmatrix} n_{ix} \\ n_{iy} \\ n_{iz} \\ 0 \end{bmatrix} = {}^{0}A_i \, {}^{i}n_i = ({}^{i}A_0)^{-1} \, {}^{i}n_i $$

$$ = \frac{s_i}{\sqrt{a_i^2 (S\beta_i)^2 + b_i^2 (C\beta_i)^2}} \begin{bmatrix} b_i I_{ix} C\beta_i C\alpha_i + b_i I_{iy} C\beta_i S\alpha_i + a_i I_{iz} S\beta_i \\ b_i J_{ix} C\beta_i C\alpha_i + b_i J_{iy} C\beta_i S\alpha_i + a_i J_{iz} S\beta_i \\ b_i K_{ix} C\beta_i C\alpha_i + b_i K_{iy} C\beta_i S\alpha_i + a_i K_{iz} S\beta_i \\ 0 \end{bmatrix} \tag{4} $$

In Figure 1, a light ray originating at point $P_{i-1} = [P_{i-1x} \quad P_{i-1y} \quad P_{i-1z} \quad 1]^T$ and directed along the unit directional vector $\ell_{i-1} = [\ell_{i-1x} \quad \ell_{i-1y} \quad \ell_{i-1z} \quad 0]^T$ is reflected/refracted at the ellipsoid medium boundary surface ${}^{i}r_i$ at point P_i. Any intermediate point Q_i along the path of the incident ray can be described parametrically as follows:

$$ Q_i = [P_{i-1x} + \ell_{i-1x}\lambda \quad P_{i-1y} + \ell_{i-1y}\lambda \quad P_{i-1z} + \ell_{i-1z}\lambda \quad 1]^T \tag{5} $$

where $\lambda \geq 0$ is the magnitude of vector $P_{i-1}Q_i$. The parameter $\lambda = \lambda_i$ corresponding to the case in which Q_i is coincident with the boundary surface at point

$$ P_i = [P_{i-1x} + \ell_{i-1x}\lambda_i \quad P_{i-1y} + \ell_{i-1y}\lambda_i \quad P_{i-1z} + \ell_{i-1z}\lambda_i \quad 1]^T \tag{6} $$

can be derived by equating the boundary surface ${}^{i}r_i$ with ${}^{i}Q_i$, where ${}^{i}Q_i = {}^{i}A_0 Q_i$ is the transformation of point Q_i to frame $(xyz)_i$, *i.e.*

$$\lambda_i = \frac{-D_i \pm \sqrt{D_i^2 - H_i \cdot E_i}}{H_i} \tag{7}$$

where H_i, D_i and E_i are given respectively by

$$H_i = \frac{1}{a_i^2} + \left(\frac{1}{b_i^2} - \frac{1}{a_i^2}\right) G_{iz}^2 \tag{8}$$

$$D_i = \frac{1}{a_i^2}(P_{i-1x}\ell_{i-1x} + P_{i-1y}\ell_{i-1y} + P_{i-1z}\ell_{i-1z}) + \left(\frac{1}{b_i^2} - \frac{1}{a_i^2}\right) B_{iz}G_{iz} + \frac{t_{ix}}{a_i^2}G_{ix} + \frac{t_{iy}}{a_i^2}G_{iy} + \frac{t_{iz}}{b_i^2}G_{iz} \tag{9}$$

$$E_i = \frac{1}{a_i^2}(P_{i-1x}^2 + P_{i-1y}^2 + P_{i-1z}^2) + \left(\frac{1}{b_i^2} - \frac{1}{a_i^2}\right) B_{iz}^2 + \frac{2t_{ix}B_{ix} + 2t_{iy}B_{iy}}{a_i^2} + \frac{2t_{iz}B_{iz}}{b_i^2} + \frac{t_{ix}^2}{a_i^2} + \frac{t_{iy}^2}{a_i^2} + \frac{t_{iz}^2}{b_i^2} - 1 \tag{10}$$

Note that in Eqs. (8) to (10), the following definitions apply:

$$B_{ix} = I_{ix}P_{i-1x} + J_{ix}P_{i-1y} + K_{ix}P_{i-1z}, \quad B_{iy} = I_{iy}P_{i-1x} + J_{iy}P_{i-1y} + K_{iy}P_{i-1z},$$

$$B_{iz} = I_{iz}P_{i-1x} + J_{iz}P_{i-1y} + K_{iz}P_{i-1z}, \quad G_{ix} = I_{ix}\ell_{i-1x} + J_{ix}\ell_{i-1y} + K_{ix}\ell_{i-1z},$$

$$G_{iy} = I_{iy}\ell_{i-1x} + J_{iy}\ell_{i-1y} + K_{iy}\ell_{i-1z}, \quad G_{iz} = I_{iz}\ell_{i-1x} + J_{iz}\ell_{i-1y} + K_{iz}\ell_{i-1z}$$

The ambiguous sign of the root term in Eq. (7) corresponds to the two possible points of intersection of the ray with the ellipsoid boundary surface. However, only one of these points is required in the current ray tracing analysis, i.e. the initial incident point, and thus the appropriate sign must be carefully chosen. The parameters α_i and β_i describing the polar angular position of the incident point on the ellipsoid boundary surface are crucial in determining the path followed by the reflected/refracted ray, and are defined as follows:

$$\alpha_i = \arctan(\rho_i, \sigma_i) \tag{11}$$

$$\beta_i = \sin^{-1}\left(\frac{\tau_i}{b_i}\right) \tag{12}$$

where $\sigma_i = B_{ix} + \lambda_i G_{ix} + t_{ix}$, $\rho_i = B_{iy} + \lambda_i G_{iy} + t_{iy}$ and $\tau_i = B_{iz} + \lambda_i G_{iz} + t_{iz}$.

In tracing the reflected/refracted ray at the ellipsoid boundary surface, the angle of incidence, θ_i, is expressed as

$$C\theta_i = -\ell_{i-1}^T \cdot n_i = \frac{-s_i}{\sqrt{a_i^2 (S\beta_i)^2 + b_i^2 (C\beta_i)^2}} (b_i G_{ix} C\beta_i C\alpha_i + b_i G_{iy} C\beta_i S\alpha_i + a_i G_{iz} S\beta_i) \quad (13)$$

According to Snell's law, the refraction angle $\underline{\theta}_i$ between two optical media is given by

$$S\underline{\theta}_i = \frac{\xi_{i-1}}{\xi_i} S\theta_i = N_i S\theta_i \quad (14)$$

where ξ_{i-1} and ξ_i are the refractive indices of media $i-1$ and i, respectively, and $N_i = \xi_{i-1}/\xi_i$ is the relative refractive index of medium $i-1$ with respect to medium i. The unit common normal vector m_i of n_i and ℓ_{i-1} can be derived as

$$m_i = [m_{ix} \quad m_{iy} \quad m_{iz} \quad 0]^T = n_i \times \ell_{i-1} / | n_i \times \ell_{i-1} | = n_i \times \ell_{i-1} / S\theta_i \quad (15)$$

According to Snell's optical law of refraction (reflection), the refracted (reflected) unit directional vector $\ell_i(\underline{\ell}_i)$ can be obtained by rotating n_i about m_i at an angle $\theta_p = \pi - \underline{\theta}_i (\theta_p = \theta_i)$ to obtain

$$\ell_i(\underline{\ell}_i) = [\ell_{ix} \quad \ell_{iy} \quad \ell_{iz} \quad 0]^T$$

$$= \begin{bmatrix} m_{ix}^2(1-C\theta_P)+C\theta_P & m_{iy}m_{ix}(1-C\theta_P)-m_{iz}S\theta_P & m_{ix}m_{iz}(1-C\theta_P)+m_{iy}S\theta_p & 0 \\ m_{iy}m_{ix}(1-C\theta_P)+m_{iz}S\theta_P & m_{iy}^2(1-C\theta_P)+C\theta_P & m_{iz}m_{iy}(1-C\theta_P)-m_{ix}S\theta_P & 0 \\ m_{ix}m_{iz}(1-C\theta_P)-m_{iy}S\theta_P & m_{iz}m_{iy}(1-C\theta_P)+m_{ix}S\theta_p & m_{iz}^2(1-C\theta_P)+C\theta_P & 0 \\ 0 & 0 & 0 & 0 \end{bmatrix} \begin{bmatrix} n_{ix} \\ n_{iy} \\ n_{iz} \\ 0 \end{bmatrix} \quad (16)$$

Further simplification of Eq. (16) is possible by utilizing the equations of $S\theta_i m_i \times n_i = (n_i \times \ell_{i-1}) \times n_i = \ell_{i-1} - (n_i^T \cdot \ell_{i-1}) n_i = \ell_{i-1} + n_i C\theta_i$ (see Eq. (15)) and the Snell's law $S\underline{\theta}_i = N_i S\theta_i$, resulting in

$$\ell_i(\underline{\ell}_i) = \begin{bmatrix} \ell_{ix} \\ \ell_{iy} \\ \ell_{iz} \\ 0 \end{bmatrix} = \begin{bmatrix} n_{ix}C\theta_P + (n_{iz}m_{iy} - n_{iy}m_{iz})S\theta_P \\ n_{iy}C\theta_P + (n_{ix}m_{iz} - n_{iz}m_{ix})S\theta_P \\ n_{iz}C\theta_P + (n_{iy}m_{ix} - n_{ix}m_{iy})S\theta_P \\ 0 \end{bmatrix} = \begin{bmatrix} n_{ix}C\theta_P + N_i(\ell_{i-1x} + n_{ix}C\theta_i) \\ n_{iy}C\theta_P + N_i(\ell_{i-1y} + n_{iy}C\theta_i) \\ n_{iz}C\theta_P + N_i(\ell_{i-1z} + n_{iz}C\theta_i) \\ 0 \end{bmatrix} \quad (17)$$

From Eq. (17), the unit directional vector of the refracted ray $\ell_i(\theta_p = \pi - \underline{\theta}_i)$ can be expressed as

$$\ell_i = \begin{bmatrix} \ell_{ix} \\ \ell_{iy} \\ \ell_{iz} \\ 0 \end{bmatrix} = \begin{bmatrix} -n_{ix}\sqrt{1-N_i^2+(N_iC\theta_i)^2} + N_i(\ell_{i-1x} + n_{ix}C\theta_i) \\ -n_{iy}\sqrt{1-N_i^2+(N_iC\theta_i)^2} + N_i(\ell_{i-1y} + n_{iy}C\theta_i) \\ -n_{iz}\sqrt{1-N_i^2+(N_iC\theta_i)^2} + N_i(\ell_{i-1z} + n_{iz}C\theta_i) \\ 0 \end{bmatrix} \tag{18}$$

while the unit directional vector of the reflected ray ℓ_i ($\theta_p = \theta_i$ and $N_i = 1$) is given by

$$\underline{\ell}_i = \begin{bmatrix} \underline{\ell}_{ix} \\ \underline{\ell}_{iy} \\ \underline{\ell}_{iz} \\ 0 \end{bmatrix} = \begin{bmatrix} \ell_{i-1x} + 2n_{ix}C\theta_i \\ \ell_{i-1y} + 2n_{iy}C\theta_i \\ \ell_{i-1z} + 2n_{iz}C\theta_i \\ 0 \end{bmatrix} \tag{19}$$

Following refraction (reflection), the light ray proceeds with point P_i as its new point of origin and ℓ_i as its new unit directional vector.

3. Error analysis at ellipsoid boundary surface

In optical systems, slight errors inevitably exist between the designed position and orientation of the optical elements and their actual position and orientation following the assembly process. In analyzing these errors, the relative positions and orientations of the world frame $(xyz)_0$ with respect to the ideal frame $(xyz)_i$ and the actual frame $(xyz)_{i'}$ can be expressed respectively as

$${}^{i}A_0 = \begin{bmatrix} I_{ix} & J_{ix} & K_{ix} & t_{ix} \\ I_{iy} & J_{iy} & K_{iy} & t_{iy} \\ I_{iz} & J_{iz} & K_{iz} & t_{iz} \\ 0 & 0 & 0 & 1 \end{bmatrix} \tag{20}$$

$${}^{i'}A_0 = \begin{bmatrix} I_{i'x} & J_{i'x} & K_{i'x} & t_{i'x} \\ I_{i'y} & J_{i'y} & K_{i'y} & t_{i'y} \\ I_{i'z} & J_{i'z} & K_{i'z} & t_{i'z} \\ 0 & 0 & 0 & 1 \end{bmatrix} \tag{21}$$

As shown in Fig. 2, the position and orientation errors of the ellipsoid boundary surface considered in the present study can be described in terms of three translational errors of the origin of frame $(xyz)_{i'}$, *i.e.*, Δx_i, Δy_i and Δz_i, and three rotational errors of the three axes of frame $(xyz)_{i'}$ with respect to frame $(xyz)_i$, *i.e.*, $\Delta\Gamma_i$, $\Delta\Psi_i$ and $\Delta\Phi_i$. The overall effect of these six errors can be expressed mathematically using a matrix ${}^{i}A_i$ of the form

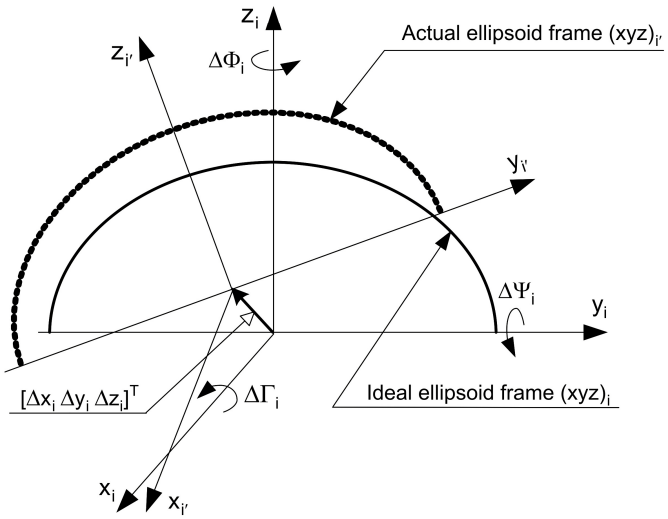

Fig. 2. Definition of translational and rotational errors of coordinate frame.

$$
{}^{i}A_{i'} = \mathrm{Trans}(\Delta x_i, \Delta y_i, \Delta z_i)\mathrm{Rot}(z_i, \Delta\Phi_i)\mathrm{Rot}(y_i, \Delta\Psi_i)\mathrm{Rot}(x_i, \Delta\Gamma_i)
$$

$$
= \begin{bmatrix}
C\Delta\Phi_i\, C\Delta\Psi_i & C\Delta\Phi_i\, S\Delta\Psi_i\, S\Delta S_i - S\Delta\Phi_i\, C\Delta\Gamma_i & C\Delta\Phi_i\, S\Delta\Psi_i\, C\Delta\Gamma_i + S\Delta\Phi_i\, S\Delta\Gamma_i & \Delta x_i \\
S\Delta\Phi_i\, S\Delta\Psi_i & S\Delta\Phi_i\, S\Delta\Psi_i\, S\Delta\Gamma_i + C\Delta\Phi_i\, C\Delta\Gamma_i & S\Delta\Phi_i\, S\Delta\Psi_i\, C\Delta\Gamma_i - C\Delta\Phi_i\, S\Delta\Gamma_i & \Delta y_i \\
-S\Delta\Psi_i & C\Delta\Psi_i\, S\Delta\Gamma_i & C\Delta\Psi_i\, C\Delta\Gamma_i & \Delta z_i \\
0 & 0 & 0 & 1
\end{bmatrix} \tag{22}
$$

Since in an optical system, the translational and rotational errors are all very small, Eq. (22) can be approximated by a first-order Taylor series expansion and rewritten in the form

$$
{}^{i}A_{i'} = \begin{bmatrix}
\bar{I}_{ix} & \bar{J}_{ix} & \bar{K}_{ix} & \bar{t}_{ix} \\
\bar{I}_{iy} & \bar{J}_{iy} & \bar{K}_{iy} & \bar{t}_{iy} \\
\bar{I}_{iz} & \bar{J}_{iz} & \bar{K}_{iz} & \bar{t}_{iz} \\
0 & 0 & 0 & 1
\end{bmatrix} = \begin{bmatrix}
1 & -\Delta\Phi_i & \Delta\Psi_i & \Delta x_i \\
\Delta\Phi_i & 1 & -\Delta\Gamma_i & \Delta y_i \\
-\Delta\Psi_i & \Delta\Gamma_i & 1 & \Delta z_i \\
0 & 0 & 0 & 1
\end{bmatrix} \tag{23}
$$

Applying the assumption that ${}^{i'}A_0 = {}^{i}A_0 + d{}^{i}A_0 = {}^{i}A_{i'}^{-1}\,{}^{i}A_0$, it can be shown that

$$
{}^{i'}A_0 = \begin{bmatrix}
I_{i'x} & J_{i'x} & K_{i'x} & t_{i'x} \\
I_{i'y} & J_{i'y} & K_{i'y} & t_{i'y} \\
I_{i'z} & J_{i'z} & K_{i'z} & t_{i'z} \\
0 & 0 & 0 & 1
\end{bmatrix} = \begin{bmatrix}
I_{ix} + \Delta I_{ix} & J_{ix} + \Delta J_{ix} & K_{ix} + \Delta K_{ix} & t_{ix} + \Delta t_{ix} \\
I_{iy} + \Delta I_{iy} & J_{iy} + \Delta J_{iy} & K_{iy} + \Delta K_{iy} & t_{iy} + \Delta t_{iy} \\
I_{iz} + \Delta I_{iz} & J_{iz} + \Delta J_{iz} & K_{iz} + \Delta K_{iz} & t_{iz} + \Delta t_{iz} \\
0 & 0 & 0 & 1
\end{bmatrix}
$$

$$= \begin{bmatrix} 1 & \Delta\Phi_i & -\Delta\Psi_i & -\Delta x_i \\ -\Delta\Phi_i & 1 & \Delta\Gamma_i & -\Delta y_i \\ \Delta\Psi_i & -\Delta\Gamma_i & 1 & -\Delta z_i \\ 0 & 0 & 0 & 1 \end{bmatrix} \begin{bmatrix} I_{ix} & J_{ix} & K_{ix} & t_{ix} \\ I_{iy} & J_{iy} & K_{iy} & t_{iy} \\ I_{iz} & J_{iz} & K_{iz} & t_{iz} \\ 0 & 0 & 0 & 1 \end{bmatrix} \tag{24}$$

From Eq. (24), it can be deduced that

$$\begin{cases} \Delta I_{ix} = I_{iy}\Delta\Phi_i - I_{iz}\Delta\Psi_i \\ \Delta I_{iy} = -I_{ix}\Delta\Phi_i + I_{iz}\Delta\Gamma_i \\ \Delta I_{iz} = I_{ix}\Delta\Psi_i - I_{iy}\Delta\Gamma_i \end{cases} \tag{25}$$

$$\begin{cases} \Delta J_{ix} = J_{iy}\Delta\Phi_i - J_{iz}\Delta\Psi_i \\ \Delta J_{iy} = -J_{ix}\Delta\Phi_i + J_{iz}\Delta\Gamma_i \\ \Delta J_{iz} = J_{ix}\Delta\Psi_i - J_{iy}\Delta\Gamma_i \end{cases} \tag{26}$$

$$\begin{cases} \Delta K_{ix} = K_{iy}\Delta\Phi_i - K_{iz}\Delta\Psi_i \\ \Delta K_{iy} = -K_{ix}\Delta\Phi_i + K_{iz}\Delta\Gamma_i \\ \Delta K_{iz} = K_{ix}\Delta\Psi_i - K_{iy}\Delta\Gamma_i \end{cases} \tag{27}$$

$$\begin{cases} \Delta t_{ix} = t_{iy}\Delta\Phi_i - t_{iz}\Delta\Psi_i - \Delta x_i \\ \Delta t_{iy} = -t_{ix}\Delta\Phi_i + t_{iz}\Delta\Gamma_i - \Delta y_i \\ \Delta t_{iz} = t_{ix}\Delta\Psi_i - t_{iy}\Delta\Gamma_i - \Delta z_i \end{cases} \tag{28}$$

Furthermore, differentiating Eqs. (6), (18) and (19), it can be shown that the differential changes in the incident point position, ΔP_i, the refracted light vector, $\Delta \ell_i$ and the reflected light vector, $\Delta \underline{\ell}_i$, are given respectively by

$$\Delta P_i = \Delta P_{i-1} + \lambda_i \Delta \ell_{i-1} + \ell_{i-1}\Delta\lambda_i = \underline{\underline{M}}_{Pi} \begin{bmatrix} \Delta P_{i-1} \\ \Delta \ell_{i-1} \end{bmatrix} + \underline{\underline{\underline{M}}}_{Pi}[\Delta e_i] \tag{29}$$

$$\Delta \ell_i = \underline{\underline{M}}_{\ell i} \begin{bmatrix} \Delta P_{i-1} \\ \Delta \ell_{i-1} \end{bmatrix} + \underline{\underline{\underline{M}}}_{\ell i}[\Delta e_i] \tag{30}$$

and

$$\Delta \underline{\ell}_i = \underline{\underline{M}}_{\underline{\ell} i} \begin{bmatrix} \Delta P_{i-1} \\ \Delta \ell_{i-1} \end{bmatrix} + \underline{\underline{\underline{M}}}_{\underline{\ell} i}[\Delta e_i] \tag{31}$$

Combining Eqs. (29), (30) and (31), the differential changes in the incident point position, ΔP_i, and the unit directional vectors of the refracted (reflected) rays, $\Delta \ell_i (\Delta \underline{\ell}_i)$, can be expressed as

$$\begin{bmatrix} \Delta P_i \\ \Delta \ell_i \end{bmatrix} = \underline{M}_i \begin{bmatrix} \Delta P_{i-1} \\ \Delta \ell_{i-1} \end{bmatrix} + \underline{\underline{M}}_i [e_i] \tag{32}$$

where $[e_i] = [\Delta x_i \;\; \Delta y_i \;\; \Delta z_i \;\; \Delta \Gamma_i \;\; \Delta \Psi_i \;\; \Delta \Phi_i]^T$. $\underline{M}_i$ is a sensitivity matrix describing the differential changes in the reflected/refracted ray unit directional vector and incident point on boundary surface r_i as a result of differential changes in the light source position and unit directional vector of the incident ray. Furthermore, $\underline{\underline{M}}_i$ is a 6×6 error matrix describing the differential changes in the reflected/refracted ray unit directional vector and incident point on boundary surface r_i induced by differential changes in the six degrees of freedom (*i.e.*, three translational and three rotational) of the frame $(xyz)_i$ of boundary surface r_i. The corresponding light path error induced at the $(n-1)$-th boundary surface can be determined from

$$\begin{aligned}
\begin{bmatrix} \Delta P_{n-1} \\ \Delta \ell_{n-1} \end{bmatrix} &= \underline{\underline{M}}_{n-1}[e_{n-1}] + \underline{M}_{n-1} \begin{bmatrix} \Delta P_{n-2} \\ \Delta \ell_{n-2} \end{bmatrix} \\
&= \underline{\underline{M}}_{n-1}[e_{n-1}] + \underline{M}_{n-1} \left\{ \underline{\underline{M}}_{n-2}[e_{n-2}] + \underline{M}_{n-2} \begin{bmatrix} \Delta P_{n-3} \\ \Delta \ell_{n-3} \end{bmatrix} \right\} \\
&= \underline{\underline{M}}_{n-1}[e_{n-1}] + \underline{M}_{n-1}\underline{\underline{M}}_{n-2}[e_{n-2}] + \underline{M}_{n-1}\underline{M}_{n-2} \begin{bmatrix} \Delta P_{n-3} \\ \Delta \ell_{n-3} \end{bmatrix} \\
&= \underline{\underline{M}}_{n-1}[e_{n-1}] + \underline{M}_{n-1}\underline{\underline{M}}_{n-2}[e_{n-2}] + \underline{M}_{n-1}\underline{M}_{n-2}\underline{\underline{M}}_{n-3}[e_{n-3}] \\
&\quad + \ldots + \underline{M}_{n-1}\underline{M}_{n-2}\underline{M}_{n-3}\underline{M}_{n-4} \ldots \underline{M}_2 \underline{\underline{M}}_1 [e_1] \\
&= M_{n-1}[e_{n-1}] + M_{n-2}[e_{n-2}] + M_{n-3}[e_{n-3}] + \ldots + M_2[e_2] + M_1[e_1].
\end{aligned} \tag{33}$$

In Eq. (33), M_i ($i = 1 \sim n-1$) is an error analysis matrix which combines the ray path errors caused by translational and rotational errors of the i-th boundary surface with the differential changes induced in the unit directional vector of the reflected/refracted ray and its incident point on the boundary surface by corresponding changes in the light source position and unit directional vector of the incident ray, *i.e.*,

$$M_i = \begin{bmatrix} \frac{\partial P_{ix}}{\partial x_i} & \frac{\partial P_{ix}}{\partial y_i} & \frac{\partial P_{ix}}{\partial z_i} & \frac{\partial P_{ix}}{\partial \Gamma_i} & \frac{\partial P_{ix}}{\partial \Psi_i} & \frac{\partial P_{ix}}{\partial \Phi_i} \\ \frac{\partial P_{iy}}{\partial x_i} & \frac{\partial P_{iy}}{\partial y_i} & \frac{\partial P_{iy}}{\partial z_i} & \frac{\partial P_{iy}}{\partial \Gamma_i} & \frac{\partial P_{iy}}{\partial \Psi_i} & \frac{\partial P_{iy}}{\partial \Phi_i} \\ \frac{\partial P_{iz}}{\partial x_i} & \frac{\partial P_{iz}}{\partial y_i} & \frac{\partial P_{iz}}{\partial z_i} & \frac{\partial P_{iz}}{\partial \Gamma_i} & \frac{\partial P_{iz}}{\partial \Psi_i} & \frac{\partial P_{iz}}{\partial \Phi_i} \\ \frac{\partial \ell_{ix}}{\partial x_i} & \frac{\partial \ell_{ix}}{\partial y_i} & \frac{\partial \ell_{ix}}{\partial z_i} & \frac{\partial \ell_{ix}}{\partial \Gamma_i} & \frac{\partial \ell_{ix}}{\partial \Psi_i} & \frac{\partial \ell_{ix}}{\partial \Phi_i} \\ \frac{\partial \ell_{iy}}{\partial x_i} & \frac{\partial \ell_{iy}}{\partial y_i} & \frac{\partial \ell_{iy}}{\partial z_i} & \frac{\partial \ell_{iy}}{\partial \Gamma_i} & \frac{\partial \ell_{iy}}{\partial \Psi_i} & \frac{\partial \ell_{iy}}{\partial \Phi_i} \\ \frac{\partial \ell_{iz}}{\partial x_i} & \frac{\partial \ell_{iz}}{\partial y_i} & \frac{\partial \ell_{iz}}{\partial z_i} & \frac{\partial \ell_{iz}}{\partial \Gamma_i} & \frac{\partial \ell_{iz}}{\partial \Psi_i} & \frac{\partial \ell_{iz}}{\partial \Phi_i} \end{bmatrix} \tag{34}$$

4. Simulation of refraction event at ellipsoid boundary surface

This section demonstrates the validity of the proposed error analysis methodology by considering the case of an optical element with an arbitrary refractive ellipsoid boundary surface. As shown in Fig. 3, it is assumed that the light source is located at a position $P_0 = [P_{0x} \quad 0 \quad -50 \quad 1]^T$ and the unit directional vector of the incoming ray has the form of either $\ell_0 = [0 \quad 0 \quad 1 \quad 0]^T$ or $\ell_0 = \left[\frac{1}{\sqrt{2}} \quad 0 \quad \frac{1}{\sqrt{2}} \quad 0\right]^T$. In addition, the ellipsoid

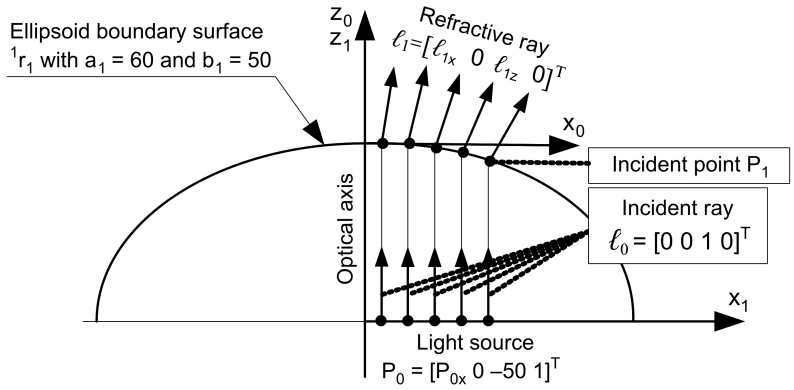

Fig. 3. Refraction process at ellipsoid boundary surface with $P_0 = [P_{0x} \quad 0 \quad -50 \quad 1]^T$ and $\ell_0 = [0 \quad 0 \quad 1 \quad 0]^T$.

boundary surface has parameters of $a_1 = 50$, $b_1 = 60$ and to the refractive index ratio the following values are assigned: $N_1 = 1.5$, $N_1 = 2.0$ or $N_1 = 2.5$. The relative configuration of the world frame $(xyz)_0$ with respect to the ellipsoid boundary surface frame $(xyz)_1$ is given by

$$ {}^{1}A_0 = \begin{bmatrix} 1 & 0 & 0 & 0 \\ 0 & 1 & 0 & 0 \\ 0 & 0 & 1 & 50 \\ 0 & 0 & 0 & 1 \end{bmatrix} \tag{35} $$

Figure 4 illustrates the variation of $\frac{\partial \ell_{1z}}{\partial x_1}$ with changes in the light source position P_{0x} as a function of the ratio of the refractive index ratio N_1. In general, it can be seen that a total reflection event occurs at small values of P_{0x}. From inspection, it is found that the value of P_{0x} associated with the total reflection phenomenon reduces as the value of the refractive index ratio N_1 increases. Moreover, it is evident that the total reflection event occurs more readily for the incident ray with a unit directional vector of $\ell_0 = [0 \;\; 0 \;\; 1 \;\; 0]^T$ than for that with a unit directional vector of $\ell_0 = \left[\frac{1}{\sqrt{2}} \;\; 0 \;\; \frac{1}{\sqrt{2}} \;\; 0\right]^T$. It can also be seen that in the case of the incident ray with a unit directional vector of $\ell_0 = [0 \;\; 0 \;\; 1 \;\; 0]^T$, a significant error exists in the path of the refractive light ray prior to the total reflection event.

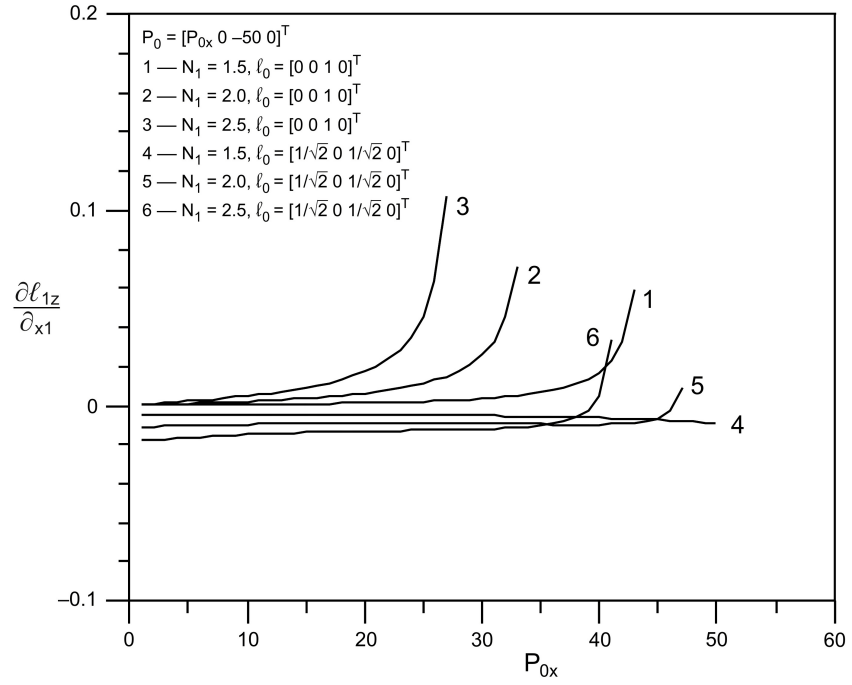

Fig. 4. Variation of $\frac{\partial \ell_{1z}}{\partial x_1}$ with light source position P_{0x} as function of refractive index ratio N_1.

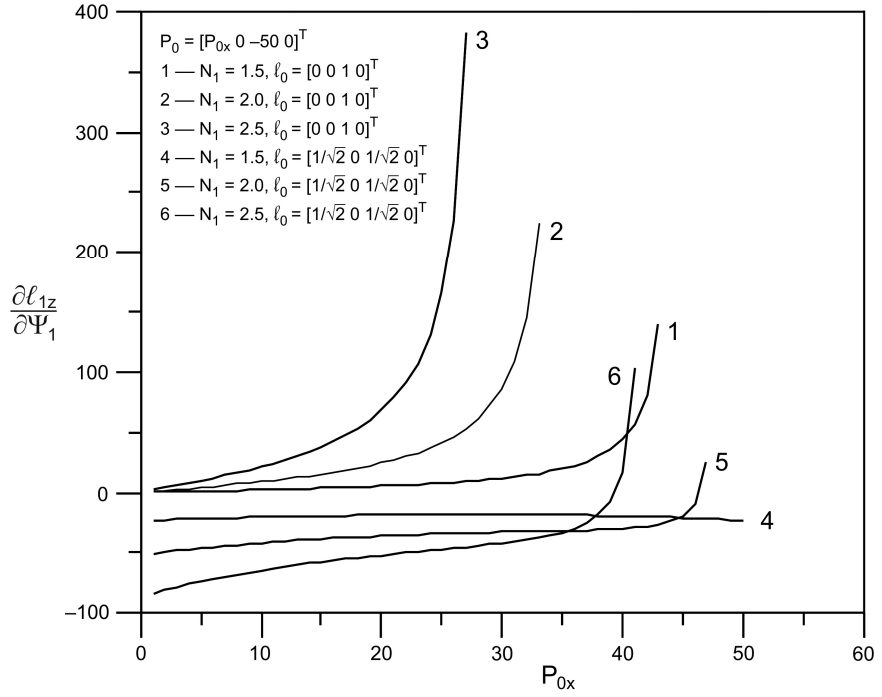

Fig. 5. Variation of $a\frac{\partial \ell_{1z}}{\partial \Psi_1}$ with light source position P_{0x} as function of refractive index ratio N_1.

Figure 5 illustrates the variation of $\frac{\partial \ell_{1z}}{\partial \Psi_1}$ with changes in the light source position P_{0x} as a function of N_1. The results clearly show that a rotational error of the boundary surface has a significant effect on the deviation of the refractive ray as the incident ray passes through the ellipsoid boundary surface. Comparing Figures 4 and 5, it is evident that a rotational error of the boundary surface has a greater effect on the deviation of the refractive ray than a translational error. Figure 6 illustrates the variation of $\frac{\partial \ell_1}{\partial P_{0x}}$ with changes in the light source position P_{0x} as a function of N_1. It is evident that the effect of ΔP_{0x} on $\Delta \ell_1$ is significantly dependent on both the value of the refractive index, N_1, and that of the unit direction vector of incoming ray, ℓ_1.

In general, Figs. 4–6 demonstrate that the orientation of the refracted light ray is significantly dependent upon the incident position of the incoming light ray and the translational and rotational errors of the boundary surface. For an incident ray with a unit directional vector of $\ell_0 = [0 \quad 0 \quad 1 \quad 0]^T$, the variation in the unit directional vector of the refracted ray, $\Delta \ell_1$, tends to zero as the position of the light source approaches the optical axis. The results have also shown that a total reflection event occurs when the light source is displaced slightly from the optical axis. This phenomenon is par-

ticularly apparent at higher values of the refractive index ratio, N_1. Overall, the results presented in Figs. 4–6 confirm the importance of performing an error analysis and then applying an appropriate calibration effect when designing optical systems comprising elements with ellipsoid boundary surfaces.

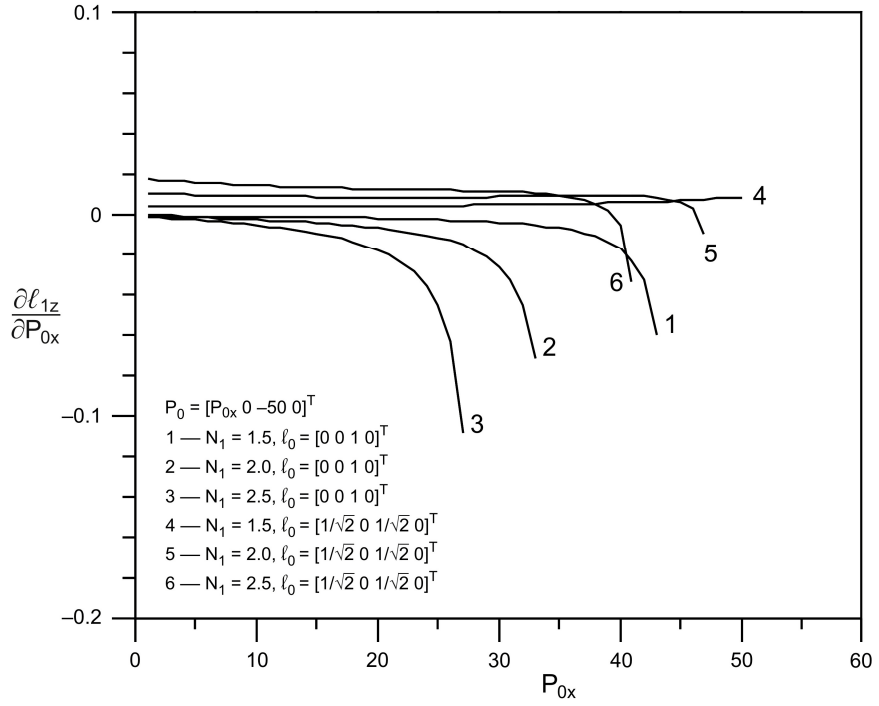

Fig. 6. Variation of $\frac{\partial \ell_1}{\partial P_{0x}}$ with light source position P_{0x} as function of refractive index ratio N_1.

5. Conclusions

This study has extended the error analysis methodology presented by the current author in [13] for optical elements with flat boundary surfaces to the case of optical components with ellipsoid boundary surfaces. The proposed methodology considers two fundamental sources of error, namely the translational and rotational errors at each boundary surface and the differential changes in the incident point position and unit directional vector of the refracted/reflected ray as a result of differential changes in the position and unit directional vector of the light source. The validity of the proposed methodology has been demonstrated by analyzing an optical element with an arbitrary ellipsoid boundary surface. In a future study, the error analysis methodology presented in this paper will be further extended to the case of optical elements with hyperbolic boundary surfaces.

Acknowledgments – The financial support provided to this study by the National Science Council of Taiwan under grant NSC96-2221-E-269-003 is gratefully acknowledged.

References

[1] SMITH W.J., *Modern Optical Engineering*, 3rd Edition, SPIE Press., McGRAW-HILL, New York 2001.
[2] BORN M., WOLF E., *Principles of Optics*, Pergamon Press, New York 1985.
[3] KINGSLAKE, R., *Lens Design Fundamentals*, Academic Press, New York 1978.
[4] FORBES G.W., *Optical system assessment for design: numerical ray tracing in the Gaussian pupil*, Journal of the Optical Society of America A, **5**(11), 1988, pp. 1943–56.
[5] FORBES G.W., *Accuracy doubling in the determination of the final ray configurations*, Journal of the Optical Society of America A, **6**(11), 1989, pp. 1776–83.
[6] STONE B.D., *Determination of initial ray configurations for asymmetric systems*, Journal of the Optical Society of America A, **14**(12), 1997, pp. 3415–29.
[7] LIAO T.T., LIN P.D., *Analysis of optical elements with flat boundary surfaces*, Applied Optics **42**(7), 2003, pp. 1191–202.
[8] LIN P.D., LU, C.H., *Analysis and design of optical system by use of sensitivity analysis of skew ray tracing*, Applied Optics **43**(4), 2004, pp. 796–807.
[9] TSAI C.Y., LIN P.D., *Prism design based on image orientation change*, Applied Optics **45**(17), 2006, pp. 3951–59.
[10] MAHAJAN V.N., *Optical Imaging and Aberrations*, SPIE Bellingham, Washington 1998.
[11] TLUSTY J., *Techniques for testing accuracy of NC-machine tools*, 12th MDTR-Conference, 1972.
[12] FERREIRA P.M., LIU R.C., *An analytical quadratic model for the geometric error of a machine tool*, Journal of Manufacturing System **5**(1), 1986, pp. 51–63.
[13] LIAO T.T., *A skew ray tracing-based approach to the error analysis of optical elements with flat boundary surfaces*, Optic 119, 2008, pp. 713–22.
[14] PAUL R.P., *Robot manipulators-mathematics*, [in:] *Programming and Control*, Cambridge, MA, 1982.

Received February 26, 2008